

Quantitative analysis by reversed-phase high-performance liquid chromatography and retinal neuroprotection after topical administration of moxonidine

Qian Zhang¹, Mei-Fang Chu¹, Yan-Hong Li², Chun-Hua Li¹, Run-Jia Lei², Si-Cen Wang³, Bao-Jun Xiao⁴, Jian-Gang Yang²

¹Department of Ophthalmology, Xi'an Fourth Hospital, Shaanxi Ophthalmological Hospital, Xi'an 710004, Shaanxi Province, China

²Xi'an Eye Hospital, First Affiliated Hospital of Northwest University; Xi'an No.1 Hospital, Xi'an 710002, Shaanxi Province, China

³School of Pharmacy, Xi'an Jiaotong University, Xi'an 710068, Shaanxi Province, China

⁴West Street Community Health Center of Lianhu District, Xi'an 710002, Shaanxi Province, China

Correspondence to: Jian-Gang Yang. Xi'an Eye Hospital, First Affiliated Hospital of Northwest University; Xi'an No.1 Hospital, Xi'an 710002, Shaanxi Province, China. jgyang0077@gmail.com

Received: 2019-03-23 Accepted: 2019-12-25

Abstract

• **AIM:** To determine moxonidine in aqueous humor and iris-ciliary body by reversed-phase high performance liquid chromatography (RP-HPLC), and to evaluate the retinal neuroprotective effect after topical administration with moxonidine in a high intraocular pressure (IOP) model.

• **METHODS:** The eyes of albino rabbits were administered topically and ipsilaterally with 0.2% moxonidine. A RP-HPLC method was employed for the identification and quantification of moxonidine between 2 and 480min, which presented in the aqueous humor and iris-ciliary body. Flash electroretinography (F-ERG) amplitude and superoxide dismutase (SOD) level were measured between day 1 and day 15 after topical administration with moxonidine in a rabbit model of high IOP. Histological and ultrastructural observation underwent to analyze the changes of retinal morphology, the inner retinal layers (IRL) thickness, and retinal ganglion cell (RGC) counting.

• **RESULTS:** Moxonidine was detectable between 2 and 480min after administration, and the peak concentration developed both in the two tissues at 30min, 0.51 µg/mL

in aqueous humor and 1.03 µg/g in iris-ciliary body. In comparison to control, F-ERG b-wave amplitude in moxonidine eyes were significantly differences between day 3 and day 15 ($P < 0.01$) in the high IOP model; SOD levels were significantly higher at all time-points ($P < 0.01$) with a maximum level of 20.29 U/mgprot at day 15; and RGCs were significantly higher ($P < 0.05$).

• **CONCLUSION:** Moxonidine is a viable neuroprotective agent with application to high IOP model. All layers of retina, including RGC layer, retinal nerve fiber layer and INL, are more preserved after moxonidine administration. SOD plays a neuroprotective role in ocular hypertension-mediated RGC death.

• **KEYWORDS:** reversed-phase high-performance liquid chromatography; moxonidine; retinal ganglion cell; neuroprotection; superoxide dismutase

DOI:10.18240/ijo.2020.03.04

Citation: Zhang Q, Chu MF, Li YH, Li CH, Lei RJ, Wang SC, Xiao BJ, Yang JG. Quantitative analysis by reversed-phase high-performance liquid chromatography and retinal neuroprotection after topical administration of moxonidine. *Int J Ophthalmol* 2020;13(3):390-398

INTRODUCTION

Moxonidine possesses a selective agonist activity at central imidazoline type-1 receptors (I1R) and a minor activity at alpha2-adrenoceptors ($\alpha 2AR$) in rostral ventrolateral medulla (RVLM) which is a main active region for control of sympathetic outflow and blood pressure^[1-3]. It is well known that moxonidine is an effective antihypertensive agent acting centrally to reduce sympathetic outflow and thus decreasing blood pressure. The agent has also been identified as an ocular hypotensive response. In previous studies, we reported that topical administration with moxonidine induced a bilateral decrease in intraocular pressure (IOP) on rabbit eyes. Mediated by peripheral $\alpha 2AR$, it was due to the increase of the uveoscleral outflow detected by immunofluorescence^[4].

Oxidative stress is mainly mediated by reactive oxygen species (ROS) generated by the metabolism of cells, such as superoxide anion, hydrogen peroxide, hydroxyl radical, and peroxynitrite. The high level of oxidative stress in RVLM contributes to increased sympathetic outflow, owing to an imbalance of generation over degradation of ROS^[5]. In a recent study, moxonidine, injected into RVLM, decreased ROS production in RVLM through the mediation of IIR^[6]. In the eye, ocular hypertension causes the death of retinal ganglion cell (RGC), a hallmark of glaucoma, suggesting that oxidative stress plays a role in RGC death in glaucoma^[7]. Recently, several literatures reported the decreased levels of ROS and lipid peroxides in experimental glaucoma eyes together with changes in the activities of antioxidant enzymes^[8-10].

Some studies demonstrated oxidative stress from mitochondrial dysfunction may play a role in glaucoma in ocular tissues derived from experimental glaucoma models and clinical samples^[11-12]. On this basis, we hypothesized that topical administration of moxonidine has an antioxidant effects, resulting in retinal neuroprotection. In the present study, we measured the concentrations in aqueous humor, iris/ciliary body and plasma with topical administration of moxonidine by reversed-phase high performance liquid chromatography (RP-HPLC) to investigate the agent pharmacokinetics. In addition, we observed the changes of the histological structure and ultrastructure of retina, counted RCG number, and analyzed the superoxide dismutase (SOD) activity to evaluate the retinal neuroprotective effect induced by moxonidine in a high IOP model.

MATERIALS AND METHODS

Ethical Approval Animal care and treatment in this study were in compliance with guidelines by the Association for Research in Vision and Ophthalmology (ARVO) resolution in the use of animals for research.

Animal The adult albino rabbits of either sex weighing 2.0-3.0 kg were used in the study. All experiments were performed at the same time of day minimizing variability related to diurnal rhythm.

Sample Preparation of Aqueous Humor, Iris-ciliary Body and Plasma Thirty-three rabbits were administered in their eyes topically and ipsilaterally with 0.2% moxonidine (Yabao Pharmaceutical, Shanxi, China) of 50 μ L by a micropipette tip, and euthanized by CO₂ inhalation at 11 time points, namely 2, 5, 10, 15, 30, 45, 60, 120, 240, 360 and 480min after moxonidine administration, respectively, 3 rabbits at each time point.

After enucleation, eyes were rinsed in phosphate buffer solution (PBS) for 5min. Aqueous humor (200 μ L) was extracted. Then the eyeballs were cut open along the limbus. The iris-ciliary bodies were removed clearly, and dried on filter

paper. The samples were precisely weighed with an analytical balance, and homogenized with 0.5 mL of a solution. All samples were stored at -20°C until used.

Reversed-phase High Performance Liquid Chromatography An RP-HPLC system (LC-10AT VP, Shimadzu, Japan) was employed for the agent concentration in the samples, consisted of a chromatographic pump and an UV detector (SPD-10AV VP). The Kromasil C18 (250 \times 4.6 mm², particle size 5 μ m) column were used. The analytical column and the guard column were operated at room temperature. The injection volume was 20 μ L. Detection was performed at 254 nm. The flow rate was set at 0.3 mL/min. The mobile phase contained methanol, water and triethylamine at ratios of 50:50:0.5.

Totally 100 μ L of 1 mol/L sodium hydroxide solution was added to 200 μ L of aqueous humor, the homogenate of iris-ciliary body, or plasma, respectively. Then 5 mL of ethyl acetate was added and mixed thoroughly by vigorous vortex mixing. After centrifugation at 4000 rpm for 5min at room temperature, 4 mL of the resultant supernatant was extracted precisely, and blow-dried with an air stream. The residue was dissolved in 200 μ L of methanol. After the second centrifugation, 50 μ L of the supernatant was injected onto the column. The peak areas measured by HPLC method were substituted into the equation of the corresponding standard curve to calculate the concentration in aqueous humor (Figure 1A). The samples of iris-ciliary body had an approximately similar retention time with aqueous humor (Figure 1B). However, the agent was not detected in plasma. For recovery tests, the samples were spiked with standard solutions of moxonidine (20 mg/L) for validation of the developed method^[13]. Extract aliquots (each 1 mL) were filtered through membrane filters (pore size: 0.2 mm) to eliminate large sized particles and subsequently analyzed by diol column coupled HPLC system. The calibration curves of analytes were established by separation of samples of concentrations at 0.05, 0.1, 0.2, 0.4, 0.6, 0.8 and 1.0 mg/L. The calibration curves were drawn by plotting the mean peak area versus analyte concentration yielded a coefficient of regression $R^2=0.9978$, with the representative linear regression equation $Y=293612X-127.37$. The linear range was between 0.002 and 0.04 μ g, and limit of quantification (LOQ) was 0.002 μ g in aqueous humor. The linear regression equation $Y=295378X-114.62$ ($R^2=0.9991$). The linear range was between 0.005 and 0.09 μ g, and LOQ was and 0.005 μ g in iris-ciliary body.

The moxonidine of different doses were added to blank aqueous humors (each 1 mL), thus producing the standard concentration of moxonidine at 0.1, 0.4 and 1.0 μ g/mL, respectively. The peak areas were measured after sample injection (10 μ L) to calculate the recovery rate of analyte,

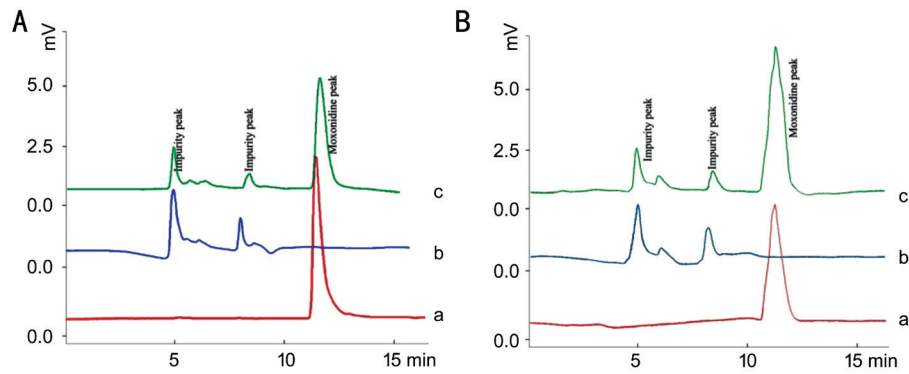


Figure 1 The typical moxonidine separation pattern in aqueous humor and iris-ciliary body on an RP-HPLC column A: The retention time of the peak in aqueous humor is measured at 12.023min. The peaks are well isolated and not overlapped. There is no interference with impurity peak. a: Standard moxonidine curve; b: An extract of blank aqueous humor; c: An extract of aqueous humor with moxonidine. B: The similar retention time in ciliary body. a: Standard moxonidine curve; b: An extract of blank iris-ciliary body; c: An extract of iris-ciliary body with moxonidine.

intraday and interday precision. The results were demonstrated in Tables 1 and 2.

Measurement of Flash Electroretinography and Superoxide Dismutase Level in High IOP Models Thirty rabbits were anesthetized with an intraperitoneal injection of a mixture of xylazine and ketamine (5 and 50 mg/kg, respectively). Under the operating microscope (66 Vision-Tech Co., Ltd, Suzhou, China), a 27-gauge needle, connected to a reservoir containing 500 mL sterile saline, was inserted into the anterior chamber of the right rabbit eye. IOP was raised to 110 mm Hg by elevating the reservoir 150 cm on the eye. Thus, the pale retina was observed by ophthalmoscopy, suggesting central retinal artery occlusion. The infusion needle was removed from the anterior chamber after 45min. The IOP may return to normal levels (Perkins applanation tonometer, Topcon SL-SD, Topcon group, Tokyo, Japan). The retinal blood flow was recovered observed by ophthalmoscopy.

The moxonidine of different doses were added to blank aqueous humors (each 1 mL), thus producing the standard concentration of moxonidine at 0.1, 0.4 and 1.0 µg/mL, respectively. The peak areas were measured after sample injection (10 µL) to calculate the recovery rate of analyte, intraday and interday precision. The results were demonstrated in Tables 1 and 2.

The animals were randomly divided into two groups, named moxonidine and control, each group of 15 rabbits. The animal models of acute high IOP were performed unilaterally. Moxonidine (0.2%) was administered topically in rabbit eye in the moxonidine group.

To evaluate functional alterations in the neuroretina, flash electroretinography (F-ERG) was taken before and after topical administration of moxonidine. UTAS-E2000 system (LKC Technologies, Gaithersburg, MD, USA) was used for ERG recordings. The recording of ERGs was performed on all

Table 1 Recovery rate of moxonidine

Concentration (µg/mL)	Observed amount (µg/µL)	Recovery (%)
0.1	0.00031±7.6×10 ⁻⁶	77.50
0.4	0.00121±4.7×10 ⁻⁶	75.63
1.0	0.00337±8.3×10 ⁻⁶	84.25

Table 2 Data for intraday and interday precision

Concentration (µg/mL)	Intraday		Interday	
	Peak area	RSD (%)	Peak area	RSD (%)
0.1	1106.38±27.36	2.47	1104.00±30.86	2.79
0.4	4298.14±165.75	3.86	4310.02±100.26	2.33
1.0	11941.06±295.01	2.47	11872.06±422.92	3.56

RSD: Relative standard deviation.

animals at baseline, day 1, 3, 7 and 15 after administration. The dark-adapted scotopic response (rod response), scotopic flash response (maximum response, cone and rod) and light-adapted photopic response (cone response) were recorded, and the b-wave amplitudes were measured. The wave amplitude ratio was calculated for the b-waves by which the responses at each time point after administration was compared with baseline.

After ERG, the rabbits were euthanized by CO₂ inhalation. The right eyes were enucleated, hemisected along the ora serata, immersed in ice saline after removing the vitreous, and everted. The retina was peeled completely, and dried on filter paper. The samples were precisely weighed with an analytical balance, then homogenized with 1% solution, and centrifuged at 300 rpm for 10min. The resultant supernatant was extracted. SOD activity was measured by hydroxylamine method^[14].

Histological and Ultrastructural Evaluation For light microscope analysis, 30 rabbits were sacrificed (2 eyes at each time point in one group). Eyes were enucleated, rinsed in PBS, and fixed in 4% paraformaldehyde. The tissue of retina

of $8 \times 10 \text{ mm}^2$ comprising optic nerve head was dehydrated, transparentized, embedded in paraffin, 5- μm thickness slices were mounted on slides, and stained with hematoxylin and eosin. RGCs were counted by high-power microscopy, and analyzed using Atomic graphs advanced software. The inner retinal layers (IRL) thickness, including retinal nerve fiber layer (RNFL), RCG layer, inner plexiform layer and inner nuclear layer, were measured.

For electron microscope, animals were sacrificed at day 7. Eyes were fixed with 0.5 L of a mixture containing 4% paraformaldehyde and 0.1% glutaraldehyde in 0.1 mol/L phosphate buffer for 30min after enucleation. The small pieces ($1 \times 1 \text{ mm}^2$) were cut near the optical nerve head, and rinsed in 2% glutaraldehyde in 0.1 mol/L cacodylate buffer (pH 7.4) at room temperature. The tissue was postfixed in 2% OsO_4 , dehydrated, and embedded in epoxy resin. Ultrathin sections were stained with uranylacetate and lead citrate, and then inspected with a transmission electron microscope.

Statistical Analysis The data were expressed as means \pm standard deviations (SD) and analyzed using IBM SPSS Statistics version 18. For comparisons among the groups, the differences in continuous data were calculated using one-way ANOVA followed by post-hoc unpaired *t*-tests. Repeated-measures ANOVA was used to compare the differences among baseline and time points. *P* values of less than 0.05 were considered statistically significant.

RESULTS

Pharmacokinetics of Moxonidine The concentration of moxonidine in the aqueous humor and iris-ciliary body after moxonidine administration is shown in Figure 2, respectively. Moxonidine was detectable in aqueous humor and iris-ciliary body at 2min after administration, 0.20 $\mu\text{g}/\text{mL}$ and 0.40 $\mu\text{g}/\text{g}$, respectively. The peak concentration developed both in the two tissues at 30min, 0.51 $\mu\text{g}/\text{mL}$ and 1.03 $\mu\text{g}/\text{g}$, respectively. It remained detected until 8h, 0.05 \pm 0.02 $\mu\text{g}/\text{mL}$ in aqueous humor and 0.22 \pm 0.16 $\mu\text{g}/\text{g}$ in iris-ciliary body. Comparison of the agent concentrations in aqueous humor and iris-ciliary body, the concentrations per unit volume in iris-ciliary body were higher than aqueous humor at each time point.

Pharmacokinetics modeling parameters were calculated by 3P97 modelling program, and the compartment modelling was automatically fit in aqueous humor and iris-ciliary body. The pharmacokinetic parameters of moxonidine showed in Table 3. The mean peak time T_{max} were 28.800 and 23.858min, and peak concentration were 0.419 $\mu\text{g}/\text{mL}$ and 0.766 $\mu\text{g}/\text{g}$ in the aqueous humor and iris-ciliary body after topical administration, respectively. The mean elimination half-life were 107.022 and 160.832min, and the mean areas under the curve (AUC) of the drug were 77.873 $\mu\text{g} \cdot \text{min}/\text{mL}$ in aqueous humor and 196.907 $\mu\text{g} \cdot \text{min}/\text{g}$ in iris-ciliary body.

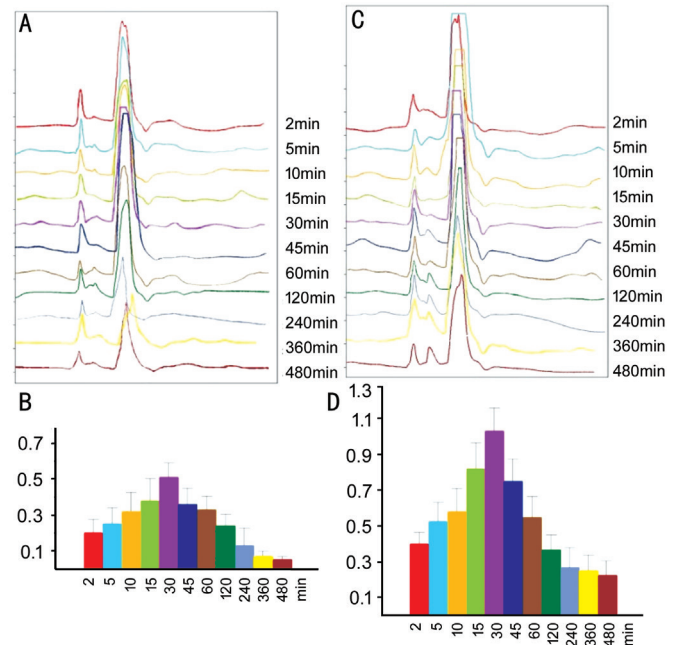


Figure 2 RP-HPLC chromatograms and mean concentrations of moxonidine in aqueous humor and iris-ciliary body from 2 to 480min after topical administration of 0.2% moxonidine eyedrop on rabbits' eyes A: RP-HPLC chromatograms in aqueous humor; B: The mean concentrations in aqueous humor, the peak concentration was 0.51 \pm 0.11 $\mu\text{g}/\text{mL}$ at 30min; C: RP-HPLC chromatograms in iris-ciliary body; D: The mean concentrations in iris-ciliary body.

Table 3 Pharmacokinetics parameters of moxonidine after topical administration of 0.2% eyedrop in rabbits

Parameters	Aqueous humor	Iris-ciliary body
K_a (/min)	0.102 \pm 0.030	0.154 \pm 0.102
K_e (/min)	0.006 \pm 0.002	0.004 \pm 0.001
$T_{1/2}K_a$ (min)	6.776 \pm 4.025	4.493 \pm 2.433
$T_{1/2}K_e$ (min)	107.022 \pm 24.624	160.832 \pm 31.490
T_{max} (min)	28.800 \pm 11.030	23.858 \pm 13.190
C_{max} ($\mu\text{g}/\text{mL}$ or g)	0.419 \pm 0.025	0.766 \pm 0.072
AUC ($\mu\text{g} \cdot \text{min}/\text{mL}$)	77.873 \pm 9.496	196.907 \pm 14.785
CL/Fs ($\text{mg} \cdot \text{kg}/\text{mL}$, $\mu\text{g}/\text{mL}$ or g)	0.0006 \pm 0.00008	0.0003 \pm 0.00005

K_a : Absorption rate constant; K_e : Elimination rate constant; $T_{1/2}K_a$: Half-life of absorption; $T_{1/2}K_e$: Half-life of elimination; T_{max} : Peak time of drug; C_{max} : Maximum concentration of drug; AUC: Area under the concentration-time curve; CL/F(s): Clearance rate.

Alteration of F-ERG b-wave Amplitude Comparison of F-ERG b-wave at baseline demonstrated no significant difference between moxonidine group and control ($P=0.462$). In control eyes, the mean recovery rate of the F-ERG b-wave amplitude maintained a relatively stable level during 15d. In comparison of control, the recovery of b-wave amplitudes in treatment eyes were significantly differences at day 3 ($P=0.001$), day 7 ($P=0.000$) and day 15 ($P=0.000$). The maximum difference between the two groups was 19.53% at day 15 (Figure 3A).

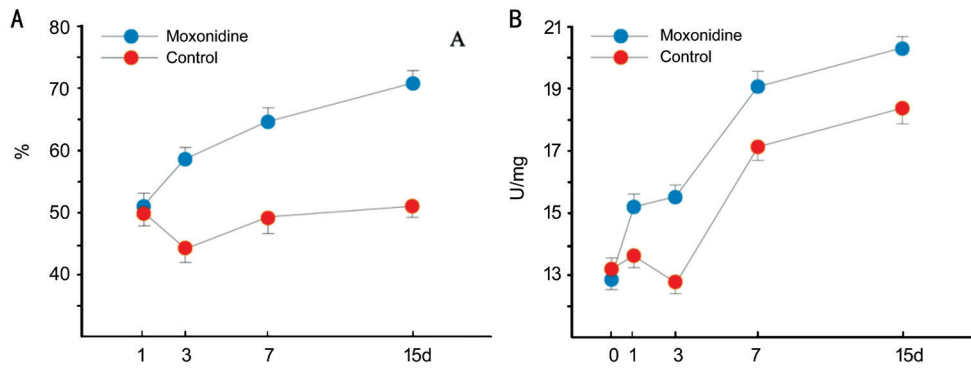


Figure 3 Comparison of amplitude recovery rate of F-ERG b-wave and SOD activities between moxonidine and control eyes A: The alteration of amplitude recovery rate of F-ERG b-wave; B: The alteration of SOD activities.

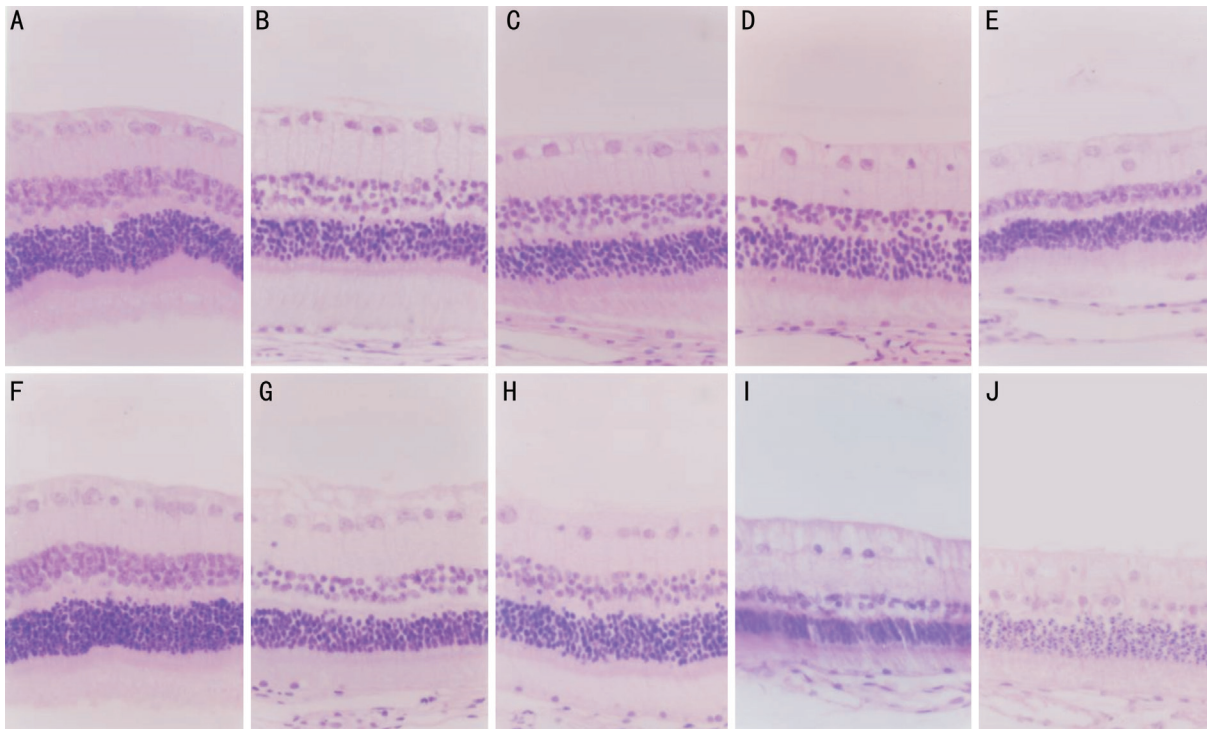


Figure 4 Hematoxylin-eosin stained retinal cross sections A-E: The retinal changes at baseline, day 1, 3, 7 and 15 in moxonidine group, respectively; F-J: The structures at the counterpart time-point in control eyes. The retinal thickness, including outer nuclear layer (ONL), inner nuclear layer (INL) and retinal nerve fiber layer (RNFL), was slightly thinned in the moxonidine-treating eyes, while much thinned in control eyes. Magnification: 400 \times .

Measurement of Retinal SOD Activity In control eyes, the low levels of SOD activities were developed at day 1 and 3. There were no significant differences compared with baseline. Then the SOD level developed a marked rise at day 7 ($P=0.000$ vs baseline), which was maintained until 15d ($P=0.000$ vs baseline). In contrast, SOD in moxonidine eyes showed an increased tendency, reaching the highest level of 20.29 U/mgprot at day 15. Furthermore, there were significant differences at all observation time-points ($P<0.01$) in comparison with baseline. Similarly, SOD activities were significantly higher than those in control eyes at all time-points after topical administration ($P<0.01$; Figure 3B).

Histological Changes With Moxonidine Administration Compared with baseline, all retinal layers were marked

swelling, and RGCs had vacuole-like change in control eyes. Then cellular edema was lightened, even disappeared. RNFLs were thinned, and RGCs were evidently lost. Subsequently, all cellular layers of retina were markedly reduced. Partial ganglion cells fragmented, dissolved and disappeared. In contrast, the swelling is much slighter originally in moxonidine eyes. Then the cell edema was gradually disappeared. All layers of retina were slightly thinned. In comparison with control, the decrease of retinal cells was less, and RGCs were less dissolved (Figure 4).

Ultrastructural Changes with Moxonidine Administration There was no difference of RGCs between moxonidine and control at baseline, consist of the typical bilayer cell membranes, round nuclei and cytoplasm with plenty of

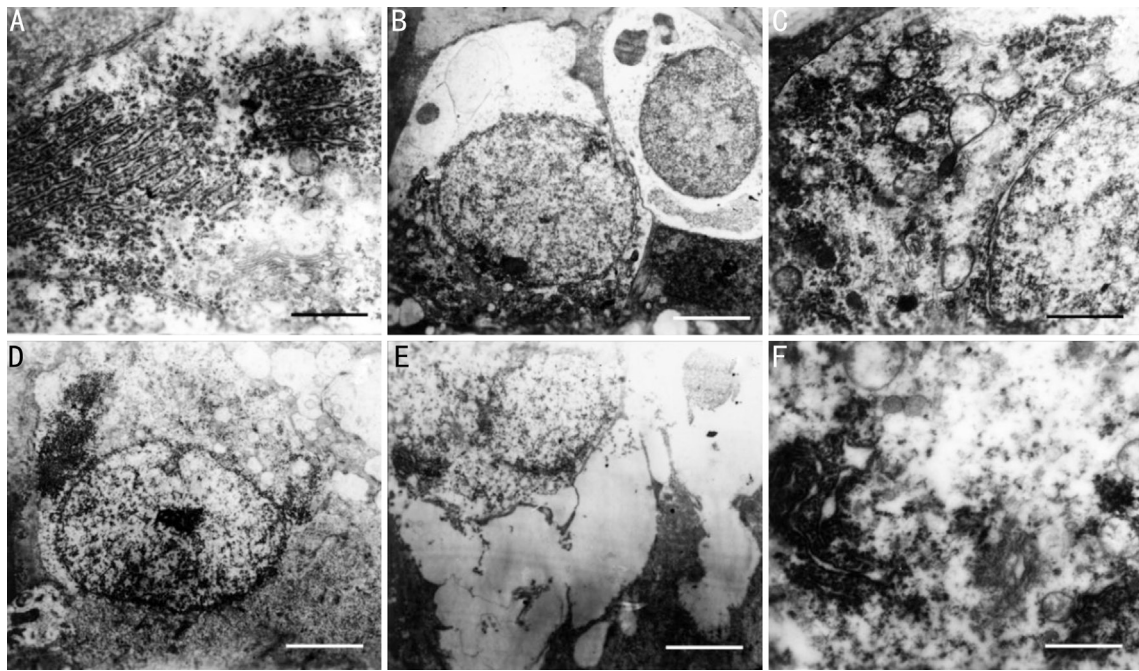


Figure 5 Transmission electron micrographs of RGCs after topical administration with moxonidine. The cell ultrastructure was treated with moxonidine (A) and placebo (D) at baseline, and with moxonidine (B and C) and placebo (E and F) at day 7 in the eyes of high IOP model. Scale bar: 0.5 μm (A, C and F) and 2 μm (B, D and E).

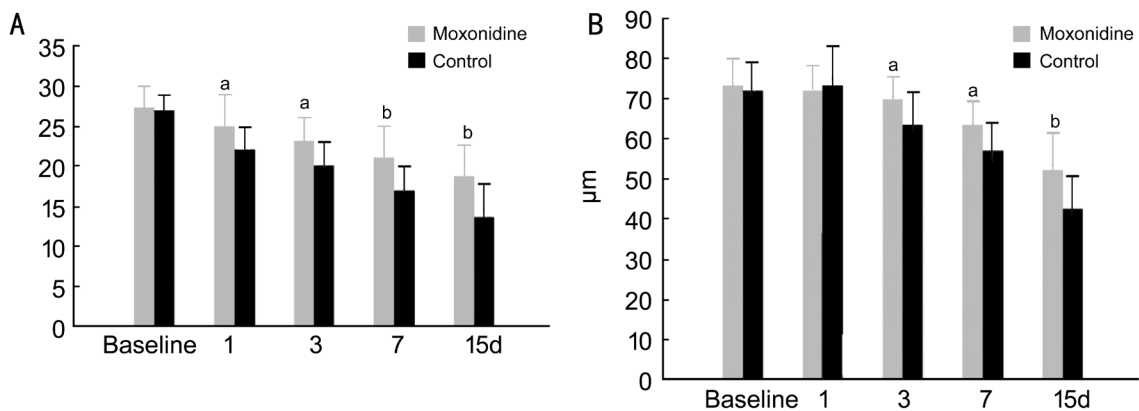


Figure 6 The RGC counting and IRL thickness between moxonidine-induced and control eyes. A: In comparison to control, there are significant increase of RGCs in moxonidine-induced eyes; B: There was difference of IRL between moxonidine-induced and control eyes. On day 1, IRLs in control eyes, because of slightly more obvious edema, were higher than those in the moxonidine-induced eyes. Whereas, IRLs in moxonidine-induced eyes were significantly higher than those in control eyes on day 3, 7 and 15. ^a $P < 0.05$; ^b $P < 0.01$.

organelles (Figure 5A and 5D). In moxonidine-induced eyes, the cell membranes were of integrity with large and round nuclei. The nucleolus and cytoplasm were dissolved slightly. The organelles showed mild swelling (Figure 5B and 5C). In control eyes, the cells were swelling with ruptured cytomembrane and chromatin margination. The organelles were dissolved to form the vacuole. The mitochondria showed high-amplitude swelling. The endoplasmic reticulum (GER) lost its granules, and Golgi complex swelled.

Ganglion Cell Counting In comparison to baseline, RGC counting decreased significantly in control eyes, 18.11% on day 1 ($P=0.006$) and 46.47% on day 15 ($P=0.000$), which presented a tendency of a longitudinal decrease. The count

also trended down in moxonidine-treated eyes though with smaller decreased amplitudes, 11.32% on day 3 ($P=0.021$) and 25.33% on day 15 ($P=0.000$). The RGCs were significantly higher in the eyes treated with moxonidine than control (Figure 6A).

Measurement of Inner Retinal Layers Thickness The IRL thickness decreased along with time in both moxonidine and placebo eyes compared with baseline. IRL decreased significantly in moxonidine-treated eyes, 3% on day 3, and 28% on day 15 ($P=0.000$), while decreased in control eyes, 13% on day 1 ($P=0.007$), and 42% on day 15 ($P=0.000$). The IRLs were significantly higher in the eyes treated with moxonidine than the control (Figure 6B).

DISCUSSION

Moxonidine plays a role in the ocular hypotensive response by a significant decrease in aqueous humor inflow and increase of uveoscleral outflow^[4]. In this study, the concentration of moxonidine was detectable of 0.20 µg/mL in aqueous humor at 2min after topical administration, meanwhile 0.40 µg/g in iris-ciliary body. The concentrations were still present at 8h both in aqueous humor and iris-ciliary body, which was in accordance with our previous study showing that the increase of aqueous humor was observed at 8-10h in the uveoscleral pathway^[4]. It suggested that moxonidine eyedrops rapidly penetrate the cornea, and reach the anterior chamber and the adjacent tissues. Furthermore, we found moxonidine concentration was more detectable in iris-ciliary body at each time point, such as the fast absorption rate, the short elimination rate constant, the long half-life of elimination, and the large AUC, indicated that the elimination rate decreased, while the absorption increased markedly.

In previous studies, the potential mechanism of moxonidine in lowering IOP was mediated by peripheral receptors in iris-ciliary body, since the activation of post-junctional vascular α 2ARs caused ciliary vasoconstriction and decreased ciliary blood flow, while activation of post-junctional epithelial α 2ARs inhibited adenylate cyclase. Thus, the high levels of moxonidine in iris-ciliary body decrease the secretion of aqueous humor, while increase the uveoscleral outflow^[4,15-16]. However, the agent was not detected in plasma, which showed that topical administration had hardly affected blood circulation in rabbits.

Oxidative stress is considered as a role in the pathogenesis of glaucoma. Several previous studies have reported lower systemic levels of antioxidants or antioxidative stress capacity in glaucoma^[12,17-18]. Nucci *et al*^[17] described that the total antioxidant capacity was decreased in aqueous humor and blood samples with primary open angle glaucoma patients. The excessive IOP, over the retinal tolerance, results in retinal ischemic/hypoxic injury, increases ROS and subsequent massive release of excitatory toxin. Ultimately it leads to the retinal tissue damage^[19-20]. The mechanisms on oxidative stress induced RGC loss in glaucoma remains unclear, but evidence shows that it is involved by direct neurotoxicity from ROS or indirect glial cell dysfunction caused by oxidative stress^[11].

Several antioxidant enzymes form the antioxidative defense system, such as SOD, catalase (CAT), paraoxonase (PON), and guaiacol peroxidase (GPX). SOD plays a major role in defense against oxidative stress *in vivo*^[21]. Initially, SOD activity was significantly decreased in an elevated IOP models in the present study, then raised gradually after 3d, and maintained up to 15d. It indicated that SOD was depleted due to the noted increase of retinal peroxides in the early stage of retinal ischemia/

reperfusion after ocular hypertension. With the prolongation of reperfusion time, SOD reactivity increased, and peroxide was gradually removed, and furthermore SOD level increased markedly. In contrast, SOD level increased significantly after moxonidine administration. This trend continued to the end of the experiment. It indicated that moxonidine reduced peroxide after ocular ischemia/reperfusion, and increased the activity of SOD. Moxonidine may slow down the ischemia progression by interfering with free radical production and oxidative stress^[22-23].

Moxonidine has a neuroprotective effect on glutamate-induced neurotoxicity to improve brain perfusion in hypertensive patients. It can increase the impaired blood flow in cerebral ischemia^[24-25]. The agent enhances the level of SOD, while reduces the elevated level of N-methyl-D-aspartic acid (NMDA). The mediation need bind to the IIR, subsequently to activate α 2AR. Several literatures demonstrated that the mechanism is also involved in the inhibition of voltage-dependent Ca_v2 current, NMDA and AMPA/kainate receptors, the influence on downstream Akt and p38 MAPK, and the activation of extracellular signal-regulated kinase (ERK) and JNK^[26-29]. However, the exact mechanism remains unclear.

F-ERG b-wave is generally believed to reflect mainly light-induced activity of bipolar cells and Muller cells, and the reaction regions of cellular electrical activity in the inner nuclear layer^[30]. In the present study, b-wave amplitude decreased in the high IOP models. Furthermore the decrease was aggravated with prolonged duration of ocular hypertension. However, b-wave amplitude increased significantly throughout the experimental period after moxonidine administration, and INL thickness was less thinned. It suggests that moxonidine relieve acute damage of visual function.

Glaucoma is a multifactorial neurodegenerative disease characterized by optic neuropathy, visual field loss, and retinal degeneration with RGC death^[31]. In this study, we found all layers of retina were thinned in the high IOP eyes, and even RGCs and RNFLs were partly disappeared. The RGCs were the most sensitive layer, then RNFLs, INLs, and last the outer layers. The RGCs were decreased by 51 % on day 15. Whereas the damage was markedly relieved by moxonidine, with a decrease of 24% at the end of experiment. RGC death in optic neuropathies is considered as a consequence of primary neuronal damage due to initial insult and secondary degeneration^[32]. The effect is attributed to the release of excitatory amino acids. Particularly glutamate release has been strongly involved in the secondary degeneration of RGC in glaucoma.

In summary, our results support moxonidine as a viable neuroprotective strategy with application to high IOP model. All layers of retina are more preserved after moxonidine

administration. INL protection is confirmed by significantly increased F-ERG b-wave amplitude. The RGC protection is verified as RGC survival by counting morphologically. Furthermore, our investigation suggests that SOD activation may play a role to achieve neuroprotection in ocular hypertension-mediated RGC death.

ACKNOWLEDGEMENTS

Foundation: Supported by the Key Science and Technology Program of Shaanxi Province, China (No.2015SF146).

Conflicts of Interest: Zhang Q, None; Chu MF, None; Li YH, None; Li CH, None; Lei RJ, None; Wang SC, None; Xiao BJ, None; Yang JG, None.

REFERENCES

- 1 Cobos-Puc LE, Aguayo-Morales H, Silva-Belmares Y, González-Zavala MA, Centurión D. A2A-adrenoceptors, but not nitric oxide, mediate the peripheral cardiac sympatho-inhibition of moxonidine. *Eur J Pharmacol* 2016;782:35-43.
- 2 Soldatov VO, Shmykova EA, Pershina MA, Ksenofontov AO, Zamitsky YM, Kulikov AL, Peresyphina AA, Dovgan AP, Belousova YV. Imidazoline receptors agonists: possible mechanisms of endothelioprotection. *Res Results Pharmacol* 2018;4(2):11-19.
- 3 Zhang LL, Ding L, Zhang F, Gao R, Chen Q, Li YH, Kang YM, Zhu GQ. Salusin- β in rostral ventrolateral medulla increases sympathetic outflow and blood pressure via superoxide anions in hypertensive rats. *J Hypertens* 2014;32(5):1059-1067; discussion 1067.
- 4 Yang JG, Sun NX, Xiong QC, Yang R. Effect of moxonidine on the uveoscleral outflow: role of alpha2-adrenoceptors or I1 imidazoline receptors. *Curr Eye Res* 2009;34(4):287-296.
- 5 Barygina V, Becatti M, Lotti T, Moretti S, Taddei N, Fiorillo C. ROS-challenged keratinocytes as a new model for oxidative stress-mediated skin diseases. *J Cell Biochem* 2019;120(1):28-36.
- 6 Wang YK, Yu Q, Tan X, Wu ZT, Zhang RW, Yang YH, Yuan WJ, Hu QK, Wang WZ. Centrally acting drug moxonidine decreases reactive oxygen species via inactivation of the phosphoinositide-3 kinase signaling in the rostral ventrolateral medulla in hypertensive rats. *J Hypertens* 2016;34(5):993-1004.
- 7 Siegfried CJ, Shui YB. Intraocular oxygen and antioxidant status: new insights on the effect of vitrectomy and glaucoma pathogenesis. *Am J Ophthalmol* 2019;203:12-25.
- 8 Saccà SC, Cutolo CA, Ferrari D, Corazza P, Traverso CE. The eye, oxidative damage and polyunsaturated fatty acids. *Nutrients* 2018;10(6):E668.
- 9 Kumar M, Tanwar M, Faiq MA, Pani J, Shamsi MB, Dada T, Dada. Mitochondrial DNA nucleotide changes in primary congenital glaucoma patients. *Mol Vis* 2013;19:220-230.
- 10 McMonnies C. Reactive oxygen species, oxidative stress, glaucoma and hyperbaric oxygen therapy. *J Optom* 2018;11(1):3-9.
- 11 Chrysostomou V, Rezanian F, Trounce IA, Crowston JG. Oxidative stress and mitochondrial dysfunction in glaucoma. *Curr Opin Pharmacol* 2013;13(1):12-15.
- 12 Yang JG, Zhou CJ, Li XY, Sun PR, Li SP, Ren BC. Alteration of UCP2 and ZO-1 expression in trabecular meshwork of neovascular glaucoma patients. *J Glaucoma* 2015;24(4):291-296.
- 13 Jonsson AS. Development and validation of a liquid chromatography-tandem mass spectrometry method for determination of cyclosporine a in whole blood. *Analytisk Kemi* 2009;121(43):7195-7204.
- 14 Guo X, Hu D, Mei X. Oxidative stress and inflammatory changes in the lung caused by cigarette smoking exposure in mice and the effect of smoking cessation. *Acta Universitatis Medicinalis Anhui* 2015;50(6):757-760.
- 15 Greenwood M, Berdahl J, Ibach M. New technology and current understanding of episcleral venous pressure. *Curr Ophthalmol Rep* 2018;6(2):86-92.
- 16 Chao HM, Osborne NN. Topically applied clonidine protects the rat retina from ischaemia/reperfusion by stimulating alpha(2)-adrenoceptors and not by an action on imidazoline receptors. *Brain Res* 2001;904(1):126-136.
- 17 Nucci C, Di Pierro D, Varesi C, Ciuffoletti E, Russo R, Gentile R, Cedrone C, Pinazo Duran MD, Coletta M, Mancino R. Increased malondialdehyde concentration and reduced total antioxidant capacity in aqueous humor and blood samples from patients with glaucoma. *Mol Vis* 2013;19:1841-1846.
- 18 Romeo Villadóniga S, Rodríguez García E, Sagastagoia Epelde O, Álvarez Díaz MD, Domingo Pedrol JC. Effects of oral supplementation with docosahexaenoic acid (DHA) plus antioxidants in pseudoexfoliative glaucoma: a 6-month open-label randomized trial. *J Ophthalmol* 2018;2018:8259371.
- 19 Crosson CE, Mani SK, Husain S, Alsarraf O, Menick DR. Inhibition of histone deacetylase protects the retina from ischemic injury. *Invest Ophthalmol Vis Sci* 2010;51(7):3639-3645.
- 20 Nita M, Grzybowski A. The role of the reactive oxygen species and oxidative stress in the pathomechanism of the age-related ocular diseases and other pathologies of the anterior and posterior eye segments in adults. *Oxid Med Cell Longev* 2016;2016:3164734.
- 21 Kim GH, Kim JE, Rhie SJ, Yoon S. The role of oxidative stress in neurodegenerative diseases. *Exp Neurobiol* 2015;24(4):325-340.
- 22 Bernatoniene J, Kopustinskiene DM. The role of catechins in cellular responses to oxidative stress. *Molecules* 2018;23(4):E965.
- 23 Rahman K. Studies on free radicals, antioxidants, and co-factors. *Clin Interv Aging* 2007;2(2):219-236.
- 24 Dojo Soeandy C, Salmasi F, Latif M, Elia AJ, Suo NJ, Henderson JT. Endothelin-1-mediated cerebral ischemia in mice: early cellular events and the role of caspase-3. *Apoptosis* 2019;24(7-8):578-595.
- 25 Gupta S, Sharma B. Pharmacological modulation of I(1)-imidazoline and α 2-adrenoceptors in sub acute brain ischemia induced vascular dementia. *Eur J Pharmacol* 2014;723:80-90.
- 26 Hayar A, Guyenet PG. Prototypical imidazoline-1 receptor ligand moxonidine activates alpha2-adrenoceptors in bulbospinal neurons of the RVL. *J Neurophysiol* 2000;83(2):766-776.

- 27 Kim YH, Nam TS, Ahn DS, Chung S. Modulation of N-type Ca²⁺ currents by moxonidine via imidazoline I1 receptor activation in rat superior cervical ganglion neurons. *Biochem Biophys Res Commun* 2011;409(4):645-650.
- 28 Poddar R, Chen A, Winter L, Rajagopal S, Paul S. Role of AMPA receptors in homocysteine-NMDA receptor-induced crosstalk between ERK and p38 MAPK. *J Neurochem* 2017;142(4):560-573.
- 29 McLean LS, Crane L, Baziard-Mouysset G, Edwards LP. Antiproliferative effect induced by novel imidazoline S43126 in PC12 cells is mediated by ROS, stress activated MAPKs and caspases. *Pharmacol Rep* 2014;66(6):937-945.
- 30 Dong CJ, Hare WA. GABA_A feedback pathway modulates the amplitude and kinetics of ERG b-wave in a mammalian retina *in vivo*. *Vision Res* 2002;42(9):1081-1087.
- 31 Krishnan A, Kocab AJ, Zacks DN, Marshak-Rothstein A, Gregory-Ksander M. A small peptide antagonist of the Fas receptor inhibits neuroinflammation and prevents axon degeneration and retinal ganglion cell death in an inducible mouse model of glaucoma. *J Neuroinflammation* 2019;16(1):184.
- 32 Levkovitch-Verbin H, Quigley HA, Martin KR, Zack DJ, Pease ME, Valenta DF. A model to study differences between primary and secondary degeneration of retinal ganglion cells in rats by partial optic nerve transection. *Invest Ophthalmol Vis Sci* 2003;44(8):3388-3393.